Single crystal elastic and thermodynamic properties of γ-$LiAlO_2$

Eiken Haussühl* and Lkhamsuren Bayarjargal
Institut für Geowissenschaften, Goethe-Universität Frankfurt, Altenhöferallee 1, D-60438 Frankfurt a.M., Germany

Javier Ruiz-Fuertes
DCITIMAC, Universidad de Cantabria, Avenida Los Castros 48, 39005 Santander, Spain
(Dated: March 9, 2021)

The elastic properties of γ-$LiAlO_2$ were reinvestigated with the aid of resonant ultrasound spectroscopy (RUS) at ambient conditions. A strong discrepancy of the elastic coefficients derived by RUS can be found from the experimental results from literature, where c_{12} and c_{13} deviate from our results by about 15 % (24 GPa) and 60 % (42 GPa), respectively. In contrast to the experimental c_{ij} from literature we can recognize a good agreement between the elastic coefficients derived from RUS and the values using density functional theory (DFT). The dielectric permittivity was measured on large plane-parellel plates and the piezoelectric stress coefficient $e_{123} = 0.14$ C m^{-2} was derived from RUS measurements at ambient conditions. The heat capacity between 4 K – 398 K has been obtained by microcalorimetry using a relaxation calorimeter. The Debye temperature was derived from heat capacity measurements ($\Theta_{\mathrm{Cp}} = 676$ K) and from RUS measurements ($\Theta_{\mathrm{elastic}} = 688$ K).

PACS numbers: Valid PACS appear here

I. INTRODUCTION

Ultraslow lithium ion conduction[1], excellent irradiation behavior and swealling resistance at elevated temperatures[2] and perfect lattice matching with III-nitrides[3] confer γ-$LiAlO_2$ single crystals the potential to be used as a substrate for growing GaN[3], as solid tritium breeder[4], or even as a CO_2 sorbent in the 500 K – 800 K range[2]. Due to the lack of inversion symmetry, it crystallizes in space group $P4_12_12$, thus showing piezoelectricity[5], with cell dimensions $a_1 = 5.169$ Å and $a_3 = 6.268$ Å[6]. In 2006, Chou *et al.*[7] reported that the acoustic velocities of γ-$LiAlO_2$ (up to 8225 m/s along the a_3 axis) are much higher than those of the currently used piezoelectric crystals, including quartz, $LiNbO_3$, and Langasite family materials, and thus γ-$LiAlO_2$ might be a potential candidate for ultrasonic device applications. However, despite the extended interest put by the scientific community since then in γ-$LiAlO_2$, one of the basic but fundamental properties of this compound remains inconsistently and sometimes incompletely determined, i. e., the elastic coefficients. The single-crystal elastic coefficients of γ-$LiAlO_2$ have been determined by several research groups[7–9] using various acoustic measurements and mostly ultrasound pulse echo techniques. However, the data are sparse and show large variations of up to 60% in the elastic coefficients c_{ij}. Considering the experimental and calculated elasticity data, the discrepancy[5,7–10] is even larger questioning the validation of the calculations or the experiments themselves. Determining sets of electromechanical coefficients of piezoelectric samples with techniques such as ultrasound pulse-echo produces inconsistency as long as they are used with differently oriented samples and with various dimensions. Especially, the accurate determination of the orientation of the samples in respect to a cartesian reference system plays an important role in obtaining the correct tensor of elasticity and piezoelectricity. In order to obtain an accurate and reliable determination of the elasticity tensor $\{c_{ij}\}$ of γ-$LiAlO_2$ we have employed resonant ultrasound spectroscopy with large-dimensions and precisely oriented single crystals. This technique, known to provide the highest accuracy has allowed us to obtain the complete set of elastic stiffness coefficients which have even helped us to derive the Debye temperature $\Theta_{\mathrm{elastic}}$ of γ-$LiAlO_2$. Furthermore, in order to check the validity of our results we have compared our c_{ij} coefficents with those calculated by several research groups[5,7–10] and the Debye temperature performing a calorimetry measurement.

II. EXPERIMENTAL DETAILS

A. Sample preparation

A large single crystal of γ-$LiAlO_2$ with a shape of a halved cylinder was provided by the Leibniz-institute for crystal growth (IKZ, Berlin, Germany) which was grown by Czochralski-techniques. The dimensions of this single crystal with optical quality were about 55 × 53 × 24 mm^3. All physical properties reported in the following are referred to a Cartesian reference system $\{\mathbf{e}_i\}$, where the axes $\mathbf{e}_i$ run parallel to those of the crystallographic reference system $\{\mathbf{a}_i\}$ (Fig. 1). For resonant ultrasound spectroscopy (RUS) experiments rectangular parallelepipeds with edges parallel to the Cartesian reference system $\{\mathbf{e}_i\}$ and edge lengths l_i of 6 mm – 11 mm (Fig. 1, table I) were cut from one large single crystal using a low-speed diamond-wire saw and were polished on glass plates using a mixture of water and Al_2O_3 powder (12 μm) and on diamond disk (mesh 3000). The sample

orientation was controlled via X-ray diffraction. The deviation from ideal orientation was kept below 0.4° and the deviation from plane-parallelism of opposing faces was smaller than ± 2 μm.

For the measurements of the dielectric permittivity of γ-$LiAlO_2$, thin plates of ca. 1.8 mm thickness and areas ranging between 8 cm^2 – 9 cm^2 were cut parallel to the crystallographic faces (100) and (001) (Fig. 1). The samples were polished flat with a deviation from plane parallelism of ± 2 μm. The large faces were covered with silver electrodes.

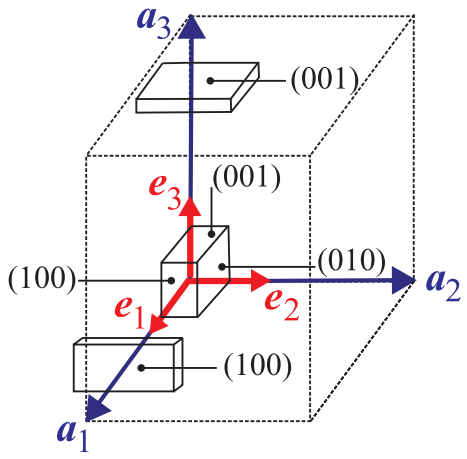

FIG. 1. Rectangular parallelepiped (main cut) used for RUS experiments and two additional oriented crystal cuts (100) and (001) in respect to a crystallographic $\{\mathbf{a}_i\}$ and Cartesian crystal-physical reference system $\{\mathbf{e}_i\}$. Dotted lines represent the tetragonal unit cell.

B. Powder X-ray diffraction

Powder X-ray diffraction was carried out to prove the phase purity and to determine the lattice parameters as well as the density being derived from the unit cell volume and the ideal chemical composition. The experiment was performed using an X'Pert Pro diffractometer from PANalytical in Bragg-Brentano geometry equipped with a PIXcel detector and Cu-$K_{\alpha 1}$ radiation. The sample was thoroughly ground in an agate mortar beforehand and mixed with silicon standard of 99.999 % purity. Both Le Bail and Rietveld refinements were carried out employing the GSAS software package. All observed reflections in the powder diffraction pattern could be indexed and no evidence of any impurity phase was found. The obtained lattice parameters a_i and the density ρ_x derived from unit cell volume and ideal chemical composition are stated in table I.

C. Heat capacity measurements

The heat capacity measurements were performed at temperatures between 4 K and 395 K using a relaxation calorimeter (heat capacity option of the Physical Properties Measurement System from Quantum Design). A single crystal with a mass of 18.22(2) mg was measured at 150 different temperatures from 395 K to 4 K with logarithmically-reduced steps. At each temperature, the heat capacity was measured three times by the relaxation method using the two-τ model[11]. The samples were thermally coupled to the sapphire holder by Apiezon N grease. The absolute accuracy of our experiments was checked by measuring the standard reference materials SRM-720 (Al_2O_3) and Cu (Alfa Aesar, 99.999 %). The deviation of our data for SRM-720 from those published by Ditmars *et al.*[12] was within 2 % in the range of 395 K to 50 K and within 6% below 5 K. The deviation of our data for Cu from those reported by Lashley *et al.*[13] was 1 % in the range from 300 K to 40 K, and 2 % below 40 K.

Molar heat capacities were fitted with polynomials of higher order to facilitate the numerical integration. The standard molar entropy $S^{\circ}_{298.15}$ and the enthalpy change between 0 K and 298.15 K, $\triangle H_{0-298.15}$, were computed with the following equations:

$$S^{\circ}_{298.15} = \int_0^{298.15} \frac{C_p}{T} dT \tag{1}$$

and

$$\triangle H_{0-298.15} = \int_0^{298.15} C_p dT. \tag{2}$$

Neglecting the difference between C_p and C_V at lower temperatures, the Debye temperature Θ_{Cp} can be determined using

$$C_V = \frac{12\pi^4}{5} nR \left(\frac{T}{\Theta_{\mathrm{Cp}}} \right)^3 \tag{3}$$

where n is the number of atoms per formula unit and $R = 8.31446$ J mol^{-1}K^{-1} [14].

D. Resonant ultrasound spectroscopy and dielectric permittivity measurements

The elastic properties were studied with the aid of RUS[15,16] using an ambient-temperature RUS-device built in-house[17–19].

The samples were clamped slightly between the ultrasound generator and the detector. The force acting on the opposed corners of the sample was kept below 0.05 N. This ensured that the experimental setup fulfilled the conditions of a nearly freely vibrating body. For signal generation and detection a network analyzer (4394A

TABLE I. Dimensions l_i of RUS-samples and densities ρ_G (calculated from dimensions and mass of RUS-samples), ρ_b (determined by buoyancy method in paraffine oil at 293 K using a large single crystal with a mass of 129.762 (1) g), ρ_x (derived from unit cell volume and ideal chemical composition), and lattice parameters a_i from powder X-ray diffraction of investigated γ-$LiAlO_2$ samples at ambient conditions.

Sample no.	1	2	3
l_1 / mm	6.675 (2)	7.163 (2)	6.844 (2)
l_2 / mm	10.242 (2)	8.421 (2)	9.032 (2)
l_3 / mm	8.559 (2)	11.130 (2)	10.017 (2)
ρ_G /g cm^{-3}	2.604 (5)	2.607 (5)	2.606 (5)
ρ_b /g cm^{-3}		2.6127 (6)	
ρ_x /g cm^{-3}		2.612 (2)	
a_1 / Å		5.1705 (2)	
a_3 / Å		6.2696 (2)	

from Keysight) was employed. On each sample (table I) at least 6 resonance spectra in the frequency range between 200 kHz and 1100 kHz with a resolution of 0.0025 kHz were collected at 295 K (Fig. 2).

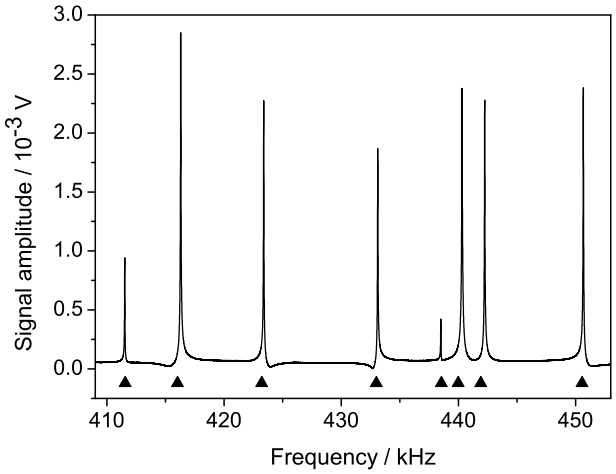

FIG. 2. Part of an experimental resonance ultrasound spectrum of a γ-$LiAlO_2$ sample (No. 3) at ambient conditions. The positions of calculated resonance frequencies are indicated by triangles.

The elastic and the piezoelectric coefficients were derived from at least 145 RUS eigen-frequencies which were recorded at room temperature. The evaluation of the six independent elastic coefficients $c_{11}, c_{12}, c_{13}, c_{33}, c_{44}, c_{66}$ and the piezoelectric stress coefficient e_{123} from the measured resonance frequencies was carried out by a nonlinear least-squares procedure in which the observed resonance frequencies were compared to those calculated from the dimensions of the sample, the experimental density, the dielectric permittivity, the piezoelectric stress coefficients and a trial set of elastic coefficients which were taken from literature[10](DFT-LDA, density functional theory, exchange correlation energy functional is treated with local density approximation). The calculated resonance frequencies were obtained by solving a general eigenvalue problem, the rank of which was equal to the number of basis functions used for the development of the components of the displacement vector. In the nonlinear least-squares refinement procedure the quantity

$$\chi^2 = \sum_{i=1}^{n} w_i \cdot (\omega_i^2(\text{calc}) - \omega_i^2(\text{obs}))^2 \qquad (4)$$

calculated for n circular eigenfrequencies with resonance frequencies $f_i = \omega_i/2\pi$ was minimized by varying the elastic coefficients c_{ij}^E at constant electric field and the piezoelectric stress coefficient e_{123} of the sample. The w_i are individual weights calculated by assuming experimental errors of ± 0.1 kHz for each observed resonance frequency. In order to minimize errors due to truncation effects, up to 8775 normalized Legendre polynomials were used in the development of the displacement vector. For extracting consistent sets of elastic and piezoelectric coefficients of piezoelectric materials it is necessary to apply the relative dielectric coefficients at constant strain $\epsilon_{11}^{\varepsilon}/\epsilon_0$ and $\epsilon_{33}^{\varepsilon}/\epsilon_0$ which were calculated from those at constant stress σ taken from literature and from experiment.

Dielectric permittivity measurements were performed at 295 K applying the geometric method to thin plane-parallel plates with arbitrary shape and a network analyzer (HP 4194 from Keysight) in a frequency range between 10 kHz and 10 MHz. For the calculation of the relative dielectric permittivity at constant stress the following equation was applied

$$\epsilon_{ii}^{\sigma}/\epsilon_0 = \frac{t^2 \rho C_{el}}{M \epsilon_0} \qquad (5)$$

where t is the thickness, ρ the density, C_{el} the capacity and M the mass of the sample, respectively. ϵ_0 denotes the permittivity of vacuum.

III. RESULTS AND DISCUSSION

Heat capacity measurements

The heat capacity of γ-$LiAlO_2$ was investigated at high temperatures above 298 K in numerous studies using drop calorimetry or a differential scanning calorimeter (DSC)[20–23]. An overview of all heat capacity results for high temperature measurements was given by Kleykamp[20]. However, there is only one study about the heat capacity of γ-$LiAlO_2$ at lower temperatures[24]. King[24] determined the heat capacity of γ-$LiAlO_2$ in the temperature range between 51 K and 298 K. In our study, we extended the temperature range down to 4 K and report the molar heat capacity C_p of γ-$LiAlO_2$ between 4 K and 393 K. The measured heat capacities were fitted in four different temperature ranges using polynomials and the fitted parameters are given in table II. The temperature ranges for fits were chosen based on a chi-squared test. The chi-square is given by $\chi^2 = \sum_{i=1}^{k}(C_p - C_{p'})^2/C_{p'}$ where C_p is the observed heat capacity and $C_{p'}$ is the expected heat capacity from the fit. Figure 3 exhibits the heat capacity data obtained here together with the results of previous studies.

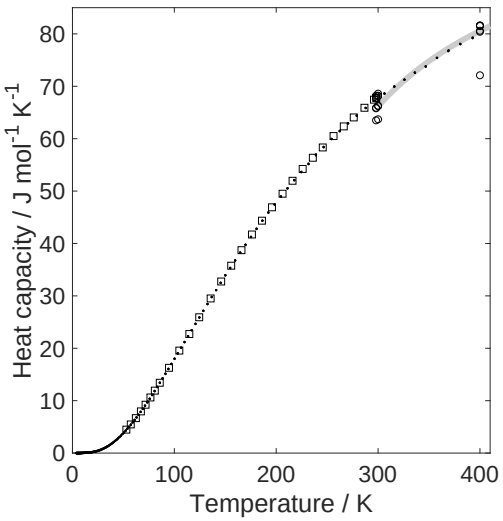

FIG. 3. The molar heat capacity C_p of γ-$LiAlO_2$ between 4 K and 390 K. Our experimental data are shown as dots and the dark line. Squares indicate data by King[24]. The thick grey line and circles represent the results by Kleykamp[20] and by references therein.

Our heat capacities are in perfect agreement with those of King[24] who measured down to 51 K. A comparison shows that our heat capacities ($C_{p,298.15K}$= 67.42 J K^{-1} mol^{-1} and $C_{p,300K}$ = 67.69 J K^{-1} mol^{-1}) at 298.15 K and 300 K agree within 1-2% with most of the previous studies. Only the result by Hollenberg and Baker[23] differs by 6% from our measurement. The computed enthalpy is $\triangle H_{0-298.15}$ = 9659 J mol^{-1} using equation 2. The computed standard entropy of γ-$LiAlO_2$ is $S^{\circ}_{298.15}$ = 53.0±0.5 J K^{-1} mol^{-1} using equation 1. This result agrees well with the value of 53.1±0.4 J K^{-1} mol^{-1} measured by King[24]. The phonon density of states and thermodynamic properties of γ-$LiAlO_2$ were computed from first-principles calculations[25] obtaining a theoretically derived entropy of 51.3 K^{-1} mol^{-1}, a value smaller than the experimental values. Our experimental data below 9 K were fitted as C_p versus T^3 using equation 3 and provide the Debye temperature θ_{Cp} = 676 K (Fig. 4). No Debye temperature has been reported before, so far.

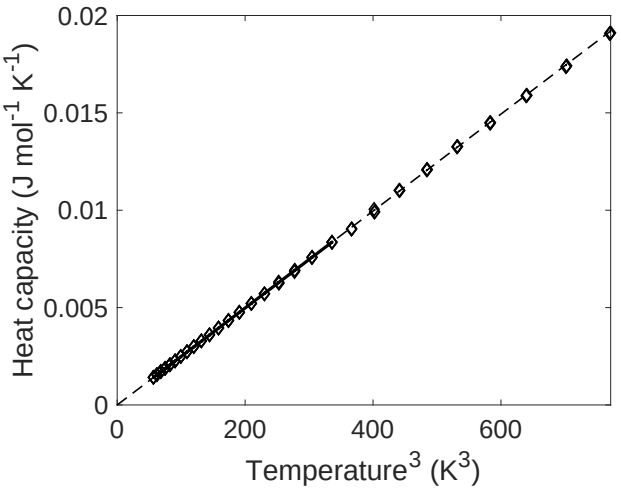

FIG. 4. Linear fit of the molar heat capacity of γ-$LiAlO_2$ for the determination of the Debye temperature (θ_{Cp} = 676 K) based on Eq. 3. Black symbols represent the measured data and the solid line the fitted function, respectively.

A. Elastic behaviour at ambient conditions

To the best of our knowledge, no RUS data of single-crystal elastic stiffness coefficients c_{ij} has been reported so far. The elastic properties of γ-$LiAlO_2$ were investigated with the aid of RUS at ambient conditions (Fig. 2). Considering that RUS provides one of the highest experimental accuracies in the determination of the c_{ij} we are confident on our data set of γ-$LiAlO_2$. The average and maximum deviations between observed and calculated resonance frequencies are about 0.25 kHz and 0.9 kHz, respectively, indicating the high accuracy of the obtained c_{ij}^{E} (measurements at constant electric field E, table III).

The single-crystal elastic stiffness coefficients of γ-$LiAlO_2$ obtained by RUS at ambient conditions are compared with those reported by various authors in table IV and in figure 5.

TABLE II. Molar heat capacities C_p of γ-$LiAlO_2$ were fitted using the polynomial function $C_p(T) = a_0 + a_1 * T + a_2 * T^2 + a_3 * T^3 + a_4 * T^4 + a_5 * T^5$. The fitted parameters a_i are given here. χ^2 is the quality parameter for the fit (for the definition see text).

temperature range	a_0	a_1	a_2	a_3	a_4	a_5	χ^2
393 K – 180 K	134.58	-2.483	0.020975	-7.6765e-05	1.3366e-07	-9.0457e-11	0.0067
180 K – 50 K	5.0678	-0.35485	0.0091352	-5.9644e-05	1.9201e-07	-2.5565e-10	0.0087
50 K – 10 K	-0.25067	0.059553	-0.0050833	0.00021	-2.6069e-06	1.2301e-08	0.0024
10 K – 4 K	-0.0036543	0.0027317	-0.00077255	0.00012805	-6.4577e-06	1.4841e-07	8.5e-06

TABLE III. Experimental elastic and electrical properties of γ-$LiAlO_2$ at ambient conditions using RUS (this study). c_{ij}^E elastic stiffness coefficients at constant electric field E. The standard deviations of the experimental c_{ij}^E as derived from the covariance matrix of the fully converged nonlinear least-squares refinements of the elastic coefficients are given in parentheses. e_{123} piezoelectric stress coefficient, d_{123} piezoelectric strain coefficient, K_{0s} adiabatic bulk modulus. g_{ii} deviation from Cauchy relations, c_{ii}^{iso} aggregate elastic coefficients (average of Voigt and Reuss model). Δf_{av} (kHz) and Δf_{max} are the average and maximum differences between measured and calculated frequencies of the eigenmodes and wR (10^{-3}) is the weighted residual of the converged refinement. ρ_b density for 293 K (determined by buoyancy method), valid for all three samples. $\epsilon_{ii}^{\sigma}/\epsilon_0$ relative dielectric permittivity at constant stress σ, $\epsilon_{ii}^{\varepsilon}/\epsilon_0$ relative dielectric permittivity at constant strain ε, measured at 1 MHz and valid for all three samples.

Sample no.	1	2	3
c_{11}^E / GPa	141.42(2)	141.64 (1)	141.69(1)
c_{12}^E / GPa	71.66 (2)	71.95 (1)	71.98(1)
c_{13}^E / GPa	70.03(1)	70.24(1)	70.16(1)
c_{33}^E / GPa	176.55 (2)	176.62 (2)	176.33 (2)
c_{44}^E / GPa	65.58(2)	65.51(5)	65.59(2)
c_{66}^E / GPa	65.68(2)	65.55(5)	65.69(2)
e_{123} / C m^{-2}	0.14(2)	0.16(1)	0.13(3)
d_{123} / pC N^{-1}	1.1 (1)	1.2 (1)	1.0(2)
K_{0s} / GPa	97.22(5)	97.44(3)	97.42(3)
$g_{11} = c_{13} - c_{44}$ / GPa	4.45	4.73	4.57
$g_{33} = c_{12} - c_{66}$ / GPa	5.98	6.40	6.29
c_{11}^{iso} / GPa	169.80	169.93	169.96
c_{44}^{iso} / GPa	54.10	54.04	54.09
No. f_{obs}	145	150	157
Δf_{av} /kHz	0.2588	0.2251	0.2337
Δf_{max} /kHz	0.8684	0.8614	0.8778
wR	0.66	0.59	0.59
ρ_b / g cm^{-3}		2.6127(6)	
$\epsilon_{11}^{\sigma}/\epsilon_0$		7.21(5)	
$\epsilon_{11}^{\varepsilon}/\epsilon_0$		7.21(5)	
$\epsilon_{33}^{\sigma}/\epsilon_0$		5.27(5)	
$\epsilon_{33}^{\varepsilon}/\epsilon_0$		5.27(5)	

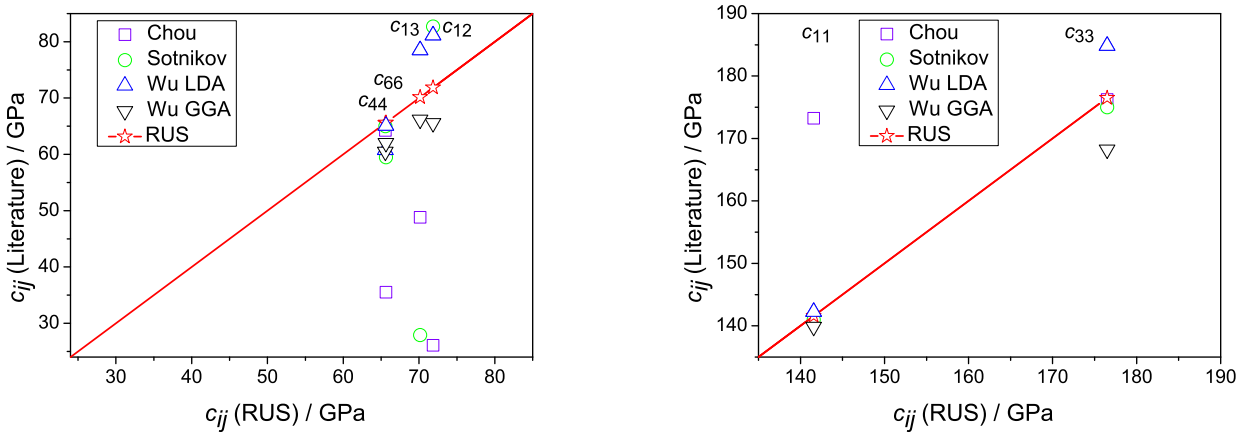

(a) (b)

FIG. 5. Elastic stiffness coefficients (a, shear and transversal elastic stiffness coefficients, b, longitudinal elastic stiffness coefficients) of γ-$LiAlO_2$ obtained from literature (Chou *et al.*[7], Sotnikov *et al.*[5] and Wu *et al.*[10 d,e]) plotted against values from RUS-experiments (this study) as a reference. The straight bisecting red line is a guide to the eye representing a correspondence between the reference data and the other data sets from literature. For the sake of clarity only data from literature comprising complete tensors of elasticity were used.

The results of this study and those by Jachmann *et al.*[8], Takagaki *et al.*[9], Chou *et al.*[7] as well as Sotnikov *et al.*[5], which were derived by experiments, differ considerably (table IV). Besides the fact that Jachmann *et al.*[8] and Takagaki *et al.*[9] published incomplete tensors of elasticity with the shear coefficients c_{44} and c_{66} missing, the deviations in c_{11} vary between ca. 5% (7 GPa) and 15% (13 GPa) and in c_{33} between 1% (2 GPa) and 10% (18 GPa) depending on the used techique where the results derived from pulse-echo technique fits best to our results[8 a]. Some of the elastic stiffness coefficients obtained from RUS are in rather poor agreement with those from Chou *et al.*[7]. The elastic stiffness coefficients c_{11}, c_{12}, c_{13} and c_{66} of Chou *et al.*[7] deviate by more than 20 % (32 GPa), 60 % (46 GPa), 30 % (21 GPa) and 45 % (30 GPa), respectively, from the results of this paper (tables III and IV). These huge differences are also clearly visible in the anisotropy of the representation surfaces of the longitudinal elastic stiffness effect (Fig. 6). In a first glance a strong discrepancy can also be found from the elastic coefficients of Sotnikov *et al.*[5], where c_{12} and c_{13} deviate from our results by about 15 % (11 GPa) and 60 % (42 GPa), respectively. In contrast to the experimental c_{ij} from literature we can recognize a good agreement between the elastic coefficients derived from RUS and the values derived from computations using density functional theory (DFT) in which the exchange correlation energy functional is treated with local density approximation (LDA)(Wu *et al.*[10 d]). Here, the maximum deviation between the elastic coefficients derived by RUS and theory (LDA) is below 13 % (9 GPa) for the transverse coefficient c_{12} (table IV).

The anistropy of the longitudinal effect, which is expressed by the ratio of the minimum and maximum of the longitudinal elastic stiffness $c'(\mathbf{u}) = u_i u_j u_k u_l c_{ijkl}$ where u_i are the direction cosines, is rather small with a value of 0.75. The maximum longitudinal elastic stiffness runs roughly along the crystallographic [111] direction (187.8 GPa), whereas the minimum can be found along [100] and [010] (141.4 GPa). It is worth to note here that the difference between the transverse coefficients c_{12} and c_{13} is about 2.5 % only and between the shear coefficients c_{44} and c_{66} it is nearly zero.

A deeper insight into the nature of bonding interactions in crystals is provided by the deviations from Cauchy relations, g_{ij}, a second-rank tensor invariant of the elasticity tensor (Haussühl[26], Schreuer and Haussühl[27]). In tetragonal crystals only the diagonal components $g_{11} = g_{22} = c_{13} - c_{44}$ and $g_{33} = c_{12} - c_{66}$ exist. In crystals with strong ionic bonds, and particularly in those containing aspherical or highly polarisable constituents, the transverse interaction coefficients dominate considerably over the corresponding shear stiffnesses resulting in positive deviations from Cauchy relations. Strong covalent or other bonds with preferential orientation usually cause opposite effects. The g_{ii} of γ-$LiAlO_2$ are all positive and in the same order of magnitude, thus indicating a 3-dimensional network of bonds dominated by Coulomb interactions. This is compatible with the analyses of Wu *et al.*[10] using DFT calculations,

where the Al–O bonding exhibits a covalent contribution, whereas the Li–O bonding is predominantly ionic.

The elastic stiffness coefficients can be used to estimate mean sound velocities which then can be employed to compute the Debye temperature according to Robie and Edwards [28]

$$\Theta_{\text{elastic}} = (h/k)[(3nN\rho)/(4\pi M)]^{1/3} v_m, \qquad (6)$$

where h and k are the Planck and Boltzmann constants, n is the number of atoms per formula unit, N is Avogadro's number, M the formula weight and v_m the mean sound velocity, respectively. A rough estimation of the mean sound velocity v_m was computed according to the approach described by Robie and Edwards [28]

$$v_m = [1/3((1/v_l^3) + (2/v_s^3))]^{-1/3}, \qquad (7)$$

where v_l and v_s are the longitudinal and shear sound velocities, respectively, using the aggregate (isotropic) elastic values c_{11}^{iso} and c_{44}^{iso} (table III, IV) derived by the Voigt-Reuss averaging. This calculation yielded $\Theta_{\text{elastic}} = 688$ K which is in good agreement with $\Theta_{\text{Cp}} = 676$ K derived from our low temperature heat capacity measurements. The relative dielectric permittivity at constant stress, $\epsilon_{ii}^{\varepsilon}/\epsilon_0$ and the extracted piezoelectric coefficient e_{123} of our work is compatible with the data from Sotnikov *et al.* [5] (table IV).

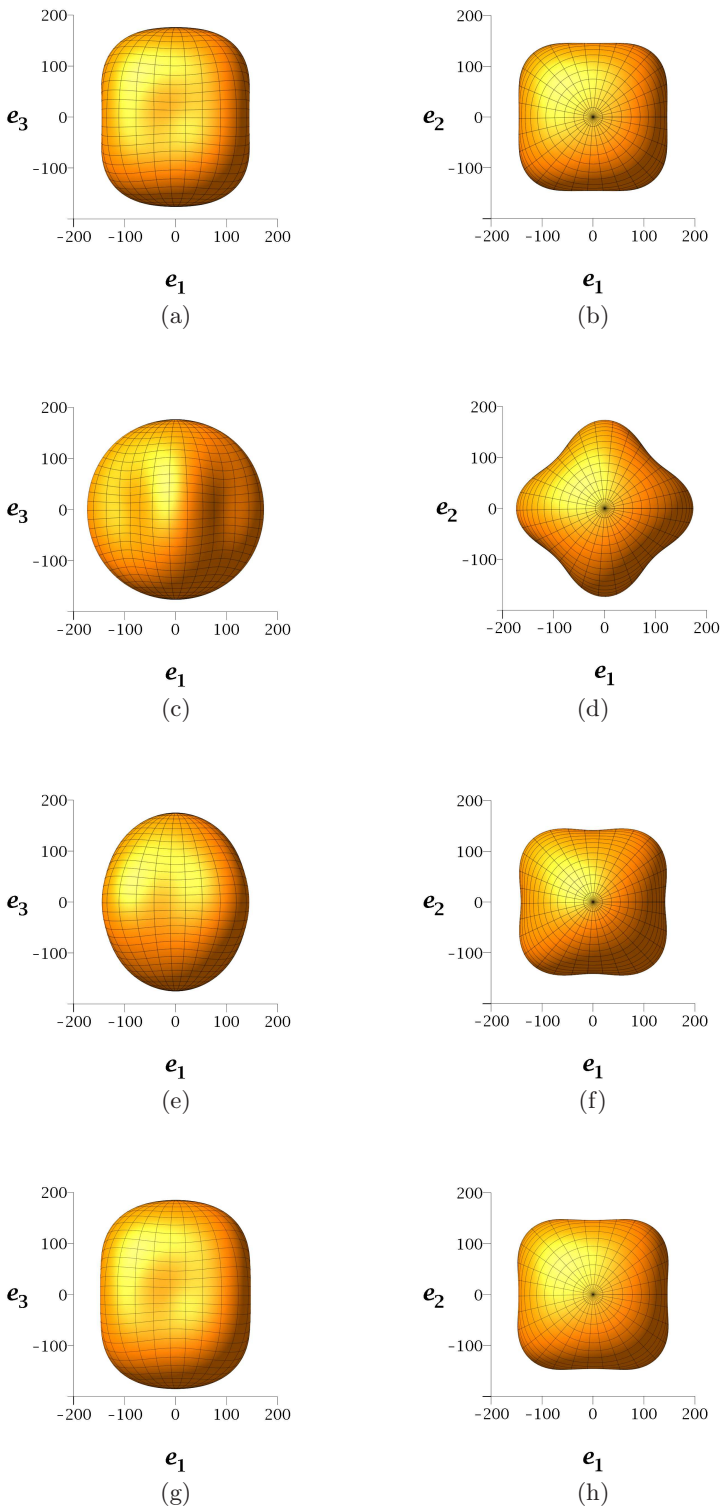

FIG. 6. Representation surfaces of the longitudinal elastic stiffness $c'_{1111} = u_{1i}u_{1j}u_{1k}u_{1l}c_{ijkl}$, units of axes are in GPa, (a–b, RUS, this work), (c–d, Chou *et al.* [7]), (e–f, Sotnikov *et al.* [5]), (g–h, Wu *et al.* [10 d]). The u_{ij} are direction cosines.

TABLE IV. Elastic properties of γ-$LiAlO_2$. c_{ij} elastic stiffness coefficients (for RUS at constant electric field E). Methods of determination of elastic stiffnesses: RUS (resonant ultrasound spectroscopy, mean values from table III), PE (pulse-echo technique), SCW_δ (sample-continuous wave technique with conventional corrections), SCW_{num} (sample-continuous wave technique with numerical corrections), SAW (surface acoustic waves), DFT-LDA (density functional theory, exchange correlation energy functional is treated with local density approximation), DFT-GGA (density functional theory, exchange correlation energy functional is treated with generalized gradient approximation) and E measurements at constant electric field (c_{ij}^E). K_{0s} adiabatic bulk modulus calculated from the c_{ij}, c_{ii}^{iso} aggregate elastic coefficients (average of Voigt and Reuss model). ρ density, $\epsilon_{ii}^\sigma/\epsilon_0$ relative dielectric permittivity at constant stress, $\epsilon_{ii}^\varepsilon/\epsilon_0$ relative dielectric permittivity at constant strain.

c_{ij}(GPa)	this study	Jachmann *et al.* [8 a]	Jachmann *et al.* [8 b]	Jachmann *et al.* [8 c]	Takagaki *et al.* [9]	Chou *et al.* [7]	Sotnikov *et al.* [5]	Wu *et al.* [10 d]	Wu *et al.* [10 e]
Method	RUS	PE	SCW_δ	SCW_{num}	SAW	PE	PE^E	DFT-LDA	DFT-GGA
Temperature	293 K						298 K	0 K	0 K
c_{11}	141.58(8)	148.49	152.19	161.84	118.0	173.24(70)	141(0.5)	142.23	139.85
c_{12}	71.86(10)	68.08	72.13	74.10	58.5	26.08(10)	82.7(1.5)	81.12	65.57
c_{13}	70.14(6)	68.73	71.72	73.87	60.2	48.83(20)	27.9(1.5)	78.50	66.16
c_{33}	176.50(8)	178.42	184.69	194.74	149.5	176.23(70)	175(0.5)	184.84	168.24
c_{44}	65.56(3)	-	-	-	-	64.27(26)	65 (0.5)	60.76	60.48
c_{66}	65.64(5)	-	-	-	-	35.53(7)	59.5(0.5)	65.09	62.04
K_{0s} / GPa	97.36(7)	-	-	-	-	85.2	81.3	103.8	93.1
c_{11}^{iso} / GPa	169.90(5)	-	-	-	-	162.1	156.0	172.0	163.0
c_{44}^{iso} / GPa	54.08(5)	-	-	-	-	57.6	55.9	50.7	52.2
e_{123} / C m^{-2}	0.14(2)	-	-	-	-	-	0.16(5)	-	-
$\epsilon_{11}^\sigma/\epsilon_0$	7.21(5)	-	-	-	-	-	-	-	-
$\epsilon_{11}^\varepsilon/\epsilon_0$	7.21(5)	-	-	-	-	-	6.8(2)	-	-
$\epsilon_{33}^\sigma/\epsilon_0$	5.27(5)	-	-	-	-	-	-	-	-
$\epsilon_{33}^\varepsilon/\epsilon_0$	5.27(5)	-	-	-	-	-	5.8(2)	-	-
ρ / g cm^{-3}	2.6127(6)	2.63	2.63	2.63	2.64	-	4.65	-	-

B. Summary

In this work, the elastic properties of γ-$LiAlO_2$ were reinvestigated with the aid of resonant ultrasound spectroscopy (RUS) at ambient conditions. We observe strong discrepancy of the elastic coefficients derived by RUS from the experimental values reported previously, i.e., where c_{12} and c_{13} deviate from our results by about 15 % (11 GPa) and 60 % (42 GPa), respectively. In contrast to the experimental c_{ij} from literature we can recognize a good agreement between the elastic coefficients derived from RUS and from computations using density functional theory (DFT). The dielectric permittivity was measured on large plane-parallel plates and the piezoelectric stress coefficient e_{123} was derived from RUS measurements at ambient conditions. The heat capacity between 4 K – 398 K has been obtained by microcalorimetry using a relaxation calorimeter. The Debye temperatures derived from sound velocities and heat capacity measurements are in good agreement within 1.7 %.

ACKNOWLEDGMENTS

The authors are grateful to J. Schreuer (Ruhr-Universität Bochum, Germany) for providing the computer program RUSREF used in the refinement of resonant ultrasound spectra. The authors gratefully acknowledge the Leibniz-institute for crystal growth (IKZ, Berlin, Germany) for the provision of a single crystal of γ-$LiAlO_2$ and the DFG for financial support of this investigation (HA 5137/3 and HA 5137/5). J.R.-F. acknowledges the MCINN (PGC2018-097520-A-100).

The data that support the findings of this study are available from the corresponding author upon reasonable request.

* haussuehl@kristall.uni-frankfurt.de

[1] D. Wiedemann, J. Nakhal, S. Rahn, E. Witt, M. M. M. Islam, S. Zander, P. Heitjans, H. Schmidt, T. Bredow, M. Wilkening, and M. Lerch, Chem. Mater. **28**, 915 (2016).
[2] Y. Duan, Micro and Nanosystems **12**, 0 (2020).
[3] P. Waltereit, O. Brandt, A. Trampert, H. T. Grahn, J. Menniger, M. Ramsteiner, M. Reiche, and K. H. Ploog, Nature **406**, 865 (2000).
[4] H. P. Paudel, Y. L. Lee, D. J. Senor, and Y. Duan, J. Phys. Chem. C **122**, 18 (2018).
[5] A. V. Sotnikov, H. Schmidt, M. Weihnacht, E. P. Smirnova, T. Chemekova, and Y. N. Yuri N. Makarov, IEEE Trans. Ultrason., Ferroel., Freq. Control **57**, 808 (2010).
[6] M. Marezio, Acta Cryst. **19**, 396 (1965).

[7] M. M. C. Chou, H. C. Huang, and Y. F. Chang, Appl. Phys. Lett. **88**, 161906 (2006).
[8] F. Jachmann, M. Pattabiraman, and C. Hucho, J. Appl. Phys. **98**, 073501 (2005).
[9] Y. Takagaki, C. Hucho, E. Wiebicke, Y. J. Sun, O. Brandt, M. Ramsteiner, and K. H. Ploog, Phys. Rev. B **69**, 115317 (2004).
[10] S. Wu, Z. Hou, and Z. Zhu, Computational Materials Science **46**, 221 (2009).
[11] C. A. Kennedy, M. Stancescu, R. A. Marriott, and M. A. White, Cryogenics **47**, 107 (2007).
[12] D. Ditmars, S. Ishihara, S. Chang, G. Bernstein, and E. West, J. Res. Natl. Bur. Stand **87**, 159 (1982).
[13] J. Lashley, M. Hundley, A. Migliori, J. Sarrao, P. Pagliuso, T. Darling, M. Jaime, J. Cooley, W. Hults, L. Morales, *et al.*, Cryogenics **43**, 369 (2003).
[14] H. Carslaw and J. Jaeger, *Heat in solids*, Vol. 1 (Clarendon Press, Oxford, 1959).
[15] R. Leisure and F. Willis, J. Phys. Condens. Matt. **9**, 6001 (1997).
[16] A. Migliori and J. Sarrao, John Wiley & Sons, New York (1997).
[17] E. Haussühl, V. L. Vinograd, T. F. Krenzel, J. Schreuer, D. J. Wilson, and J. Ottinger, Z. Kristallogr. **226** (2011).
[18] E. Haussühl, J. Schreuer, B. Winkler, S. Haussühl, L. Bayarjargal, and V. Milman, J. Phys. Condens. Matt. **24**, 345402 (2012).
[19] E. Haussühl, H. J. Reichmann, J. Schreuer, A. Friedrich, C. Hirschle, L. Bayarjargal, B. Winkler, I. Alencar, L. Wiehl, and S. Ganschow, Mater. Res. Express **7**, 025701 (2020).
[20] H. Kleykamp, Journal of nuclear materials **270**, 372 (1999).
[21] M. Asou, T. Terai, and Y. Takahashi, Journal of nuclear materials **175**, 42 (1990).
[22] R. Brandt and B. Schulz, Journal of Nuclear Materials **152**, 178 (1988).
[23] G. Hollenberg and D. Baker, Hanford Engineering Development Laboratory (1982).
[24] E. King, Journal of the American Chemical Society **77**, 3189 (1955).
[25] S.-G. Ma, Y.-H. Shen, T. Gao, and P.-H. Chen, International Journal of Hydrogen Energy **40**, e3770 (2015).
[26] S. Haussühl, Phys. kond. Mat. **6**, 181 (1967).
[27] J. Schreuer and S. Haussühl, EMU Notes in Mineralogy **7**, 173 (2005).
[28] R. A. Robie and J. L. Edwards, J. Appl. Phys. **37**, 2659 (1966).